University of Tennessee, Knoxville
Trace: Tennessee Research and Creative Exchange

Chemical and Biomolecular Engineering Publications and Other Works

Chemical and Biomolecular Engineering

1-1-2009

SELF-CONSISTENT MULTISCALE MODELING IN THE PRESENCE OF INHOMOGENEOUS FIELDS

David Keffer
University of Tennessee - Knoxville, dkeffer@utk.edu

Follow this and additional works at: http://trace.tennessee.edu/utk_chembiopubs

Part of the Complex Fluids Commons, Membrane Science Commons, Nanoscience and Nanotechnology Commons, Polymer Science Commons, Thermodynamics Commons, and the Transport Phenomena Commons

Recommended Citation
Keffer, David, "SELF-CONSISTENT MULTISCALE MODELING IN THE PRESENCE OF INHOMOGENEOUS FIELDS" (2009). *Chemical and Biomolecular Engineering Publications and Other Works.*
http://trace.tennessee.edu/utk_chembiopubs/1

This Article is brought to you for free and open access by the Chemical and Biomolecular Engineering at Trace: Tennessee Research and Creative Exchange. It has been accepted for inclusion in Chemical and Biomolecular Engineering Publications and Other Works by an authorized administrator of Trace: Tennessee Research and Creative Exchange. For more information, please contact trace@utk.edu.

MULTISCALE MODEL. SIMUL.
Vol. 8, No. 1, pp. 193–203
© 2009 Society for Industrial and Applied Mathematics

SELF-CONSISTENT MULTISCALE MODELING IN THE PRESENCE OF INHOMOGENEOUS FIELDS*

RUICHANG XIONG†, REBECCA L. EMPTING†, IAN C. MORRIS†, AND DAVID J. KEFFER†

Abstract. Molecular dynamics (MD) simulations of a Lennard–Jones fluid in an inhomogeneous external field generate steady-state profiles of density and pressure with nanoscopic heterogeneities. The continuum level of mass, momentum, and energy transport balances is capable of reproducing the MD profiles only when the equation of state for pressure as a function of density is extracted directly from the molecular level of description. We show that the density profile resulting from simulation is consistent with both a molecular-level theoretical prediction from statistical mechanics as well as the solution of the continuum-level set of differential equations describing the conservation of mass and momentum.

Key words. molecular dynamics, inhomogeneous fluid, multiscale modeling, thermostat

AMS subject classification. 81V55

DOI. 10.1137/080741963

1. Introduction.

The principles of conservation of mass, momentum, and energy in classical systems are equally valid at both the continuum and the molecular levels. At the continuum level, the density and velocity distributions are given by solutions of partial differential equations (PDEs) describing the mass and momentum balances. It is sufficient for the purposes of this work to limit the investigation to single-component fluids in an isothermal system. Therefore, the relevant continuum equations are a mass balance [1],

$$\frac{\partial \rho}{\partial t} = -\nabla \cdot (\rho v), \tag{1a}$$

where ρ is the mass density, $\mathbf{v}$ is the center-of-mass velocity, and t is time, and a momentum balance,

$$\rho \frac{\partial \mathbf{v}}{\partial t} = -\rho \mathbf{v} \cdot \nabla(\mathbf{v}) - \nabla p - \nabla \cdot \boldsymbol{\tau} - \rho \nabla \hat{\Phi}, \tag{1b}$$

where p is the hydrostatic pressure, $\boldsymbol{\tau}$ is the extra stress tensor, and $\hat{\Phi}$ is an external field. These PDEs require a constitutive equation providing the functional form of the extra stress tensor, $\boldsymbol{\tau}$, e.g., Newton's law of viscosity, as well as a thermodynamic constitutive equation providing the functional form of the pressure, p, e.g., a mechanical equation of state such as the van der Waals equation of state (EOS) or

*Received by the editors November 26, 2008; accepted for publication (in revised form) March 2, 2009; published electronically November 25, 2009. This research was supported by the donors of the Petroleum Research Fund, administered under grant 42201-AC9. This research project also used resources of the Center for Computational Sciences at Oak Ridge National Laboratory, which is supported by the Office of Science of the Department of Energy under contract DE-AC05-00OR22725.
The U.S. Government retains a nonexclusive, royalty-free license to publish or reproduce the published form of this contribution, or allow others to do so, for U.S. Government purposes. Copyright is owned by SIAM to the extent not limited by these rights.
http://www.siam.org/journals/mms/8-1/74196.html
†Department of Chemical and Biomolecular Engineering, University of Tennessee, 1512 Middle Drive, Knoxville, TN 37996-2200 (rxiong@utk.edu, rempting@utk.edu, imorris@utk.edu, dkeffer@utk.edu).

Copyright © by SIAM. Unauthorized reproduction of this article is prohibited.

the Lennard–Jones EOS [2]. With a set of boundary conditions, this set of PDEs and constitutive equations can readily be solved.

At the molecular level, these same principles apply. In a traditional equilibrium molecular dynamics (EMD) simulation, there are no gradients in the system and principles of mass and momentum conservation reduce to the number of particles and total system momentum being invariant in time. In a nonequilibrium molecular dynamics (NEMD) simulation in the presence of an inhomogeneous, external field, it is possible to generate gradients in the density and velocity profiles. Because of the resolution of molecular dynamics (MD) simulations, these gradients can easily be on the order of nanometers. In this case, the mass and momentum balances of (1) are completely valid and should be observed in the simulation. The only issue is that the constitutive equations for both $\boldsymbol{\tau}$ and p must now be valid in the presence of nanoscale inhomogeneities.

In general, constitutive equations developed for bulk fluids (both for transport and thermodynamic properties) are not valid in the presence of nanoscale inhomogeneities. Therefore, it is necessary to extract these constitutive equations from the molecular-level models in order to show consistency between the density and velocity profiles obtained through the solution of the continuum-level equations and the profiles directly observed in the simulation.

Molecular-level information in the presence of inhomogeneous fields can be generated in a variety of ways, including molecular density functional theory (DFT), integral equation theory (IET), and molecular simulation (both Monte Carlo methods and molecular dynamics) [3]. In previous multiscale modeling work we have used the Ornstein–Zernike IET to provide molecular information used in continuum-level models [4]. In this work, we choose to generate the molecular-level information from MD simulations.

We perform MD simulations in the presence of an inhomogeneous field to generate time-invariant density profiles with variation on the nanoscale. We directly evaluate the pressure profile in the MD simulations and use it to create a mechanical EOS that relates pressure to density for this particular inhomogeneous fluid. When this EOS is substituted into the continuum-level equations, we find that the macroscopic model reproduces the density profiles from the molecular-level simulation. We also show that neither a bulk mechanical EOS nor local averaging of the bulk EOS reproduces the MD results.

The systems of study include both the ideal gas, for illustrative purposes, and the Lennard–Jones fluid. For the ideal gas, it became necessary to develop a new thermostat for the MD systems with inhomogeneous fields. To this end, we developed, applied, and validated this thermostat through comparison with statistical mechanical and continuum-level theory.

This work demonstrates several important issues associated with multiscale modeling. First, concepts such as the conservation of mass, momentum, and energy should be equally applicable at all scales. The failure of (1) to describe observed density, momentum, or temperature profiles at the molecular level is due to the use of constitutive equations that are not valid at the nanoscale. Finally, when comparing the continuum-level and molecular-level systems, all profiles—mass, momentum, and temperature—must simultaneously agree between the scales. This may require the development of new simulation nuances, such as a novel thermostat, as was the case in this work.

The remainder of this work is organized as follows. In section 2, we provide the

Copyright © by SIAM. Unauthorized reproduction of this article is prohibited.

necessary background to explain and justify the new thermostat. In section 3, we present results of the MD simulations. In section 4, we provide our conclusions.

2. System formulation. The study of temperature control in MD simulation has received an extensive amount of interest since the early work of Nosé [5] and Hoover [6] through more recent analyses and descriptions of families of thermostat formalisms [7, 8, 9, 10, 11, 12]. One of the salient features of these thermostats is their application to selective degrees of freedom, allowing, for example, a distinct thermostat of light and heavy particles [8] or an exclusive thermostat of the peculiar momentum [11].

In this work, we are interested in thermostatting MD simulations in the presence of an arbitrary and potentially anisotropic and spatially inhomogeneous field. The field will generally give rise to inhomogeneous distributions in the density, center-of-mass velocity, and temperature. We are interested in performing simulations in an isothermal limit, in which the temperature is constant throughout the simulation volume. For a Lennard–Jones fluid in which there is exchange of kinetic energy between particles through collisions, a single Nosé–Hoover thermostat will suffice. For an ideal gas, we demonstrate the implementation of a set of Nosé–Hoover thermostats that will provide a spatially uniform temperature distribution. Furthermore, we justify the implementation of the thermostat not only through direct examination of the temperature distribution but also through comparison of the resulting inhomogeneous density distributions with profiles predicted from both statistical mechanics as well as continuum mass and momentum balances evaluated in the isothermal limit.

In order to validate our thermostat, we require standards for comparison. There are various levels of validation that can be checked. First and most obviously, the average temperature of the simulation must be correctly maintained. Second, the spatial temperature distribution must correspond to the set temperature distribution. These criteria for a successful thermostat are, however, insufficient to prove the rigor of the procedure.

We require an additional criterion in order to provide evidence that the means by which the uniform profile was obtained did not disturb other results of the simulation. In the absence of any inhomogeneous fields, this additional proof is given by the Hamiltonian-based criterion used by Nosé [13] or the non-Hamiltonian criterion of Tuckerman et al. [14, 15]. However, the inhomogeneous field will give rise to a density distribution. In this work, we use the density distribution as a criterion for the success of the thermostat by comparing the density distribution from the MD simulations with two standards. For the simulations of the ideal gas, we can compare the density distribution with that predicted by statistical mechanics. The density distribution, $\rho(z)$, of the ideal gas in the presence of an external field is given by the statistical mechanical result

$$\rho(z) = \rho_o \exp\left(\frac{\hat{\Phi}(z)}{k_B T}\right), \tag{2}$$

where ρ_o is a constant, k_B is Boltzmann's constant, T is temperature, $\hat{\Phi}$ is the external potential, and z is the spatial dimension.

For both the ideal gas and the Lennard–Jones fluid, we can validate density distributions from the MD simulations through a multiscale modeling algorithm. Namely, the density distribution that is the solution to the continuum level mass and momentum balances in (1) should directly match the profiles from the MD simulations. It

Copyright © by SIAM. Unauthorized reproduction of this article is prohibited.

is important to understand that, without coupling to an energy balance, (1) assumes that the system is isothermal. Therefore, if the continuum-level system is isothermal, then so too must be the molecular-level system.

It is completely sufficient for our purposes to focus on steady-state solutions in which the time derivatives in (1) are zero. Furthermore, we will examine an anisotropic external field with variation in the z-direction only. We choose the boundary condition for the velocity to be zero, thus essentially setting the velocity profile to zero and eliminating the convection and dissipation term from (1). Consequently, our system of equations becomes

$$\frac{dp}{dz} = -\rho \frac{d\hat{\Phi}}{dz}. \tag{3}$$

We are free to choose any arbitrary form of the external potential. In our examples, we choose the external field to be a time-invariant cosine function with a spatial period equal to the system size in the z-dimension, L, specifically $\hat{\Phi} = A\cos(2\pi\, z/L)$. This choice is motivated by the fact that we would greatly prefer that the density profile satisfying the continuum equations be periodic. This will allow the corresponding MD simulations to achieve steady state using traditional periodic boundary conditions. (There are no simple boundary conditions that would allow MD simulations to be performed if, for example, the density at one boundary of the box were different from the density at the opposite boundary. In such a case, a technique such as dual-control-volume grand canonical MD would be required [16].) In the case of negligible velocity profile, the choice of a periodic external potential is sufficient to generate a periodic density profile.

At the molecular level, we perform an MD simulation, which is an equilibrium simulation in every respect except that the external field, $\hat{\Phi}$, is present in the z-dimension. We therefore expect that an MD simulation with a correct thermostat will generate the same density profile as that obtained from the continuum description, given that we have a reasonable EOS for the pressure in the continuum model.

It is worth noting that, in general, the presence of the inhomogeneous field will give rise to variations in density, velocity, and temperature. If there is variation in the velocity, then one would call these simulations "nonequilibrium molecular dynamics" (NEMD) simulations. Based on our specific choice of boundary conditions in the continuum model for this example, we have negligible variation in the velocity, and thus our MD simulations are "equilibrium molecular dynamics with an inhomogeneous potential."

The MD simulations used 10,000 molecules at temperature of 300 K and 150 K, respectively, and a molecular volume of 100 Å^3/molecule. We used the Lennard–Jones potential [17], truncated at a cut-off of 15 Å, with $\varepsilon/k_B = 93.10$ K, $\sigma = 3.446$ Å, and molecular weight 39.948 g/mole. For the ideal gas simulations, we set ε to zero. The time step was 10 fs. Equilibration and data collection were performed for 7.5 and 10.0 ns, respectively. We used the fifth-order gear predictor-corrector method to integrate the equations of motion [18, 19], which has been shown to provide excellent conservation of the Hamiltonian in MD simulations [17].

We present results comparing the molecular and continuum models for two systems: An ideal gas and a Lennard–Jones fluid. The essential difference between the ideal gas and a Lennard–Jones fluid is that the ideal gas lacks any intermolecular interaction. We will see the consequence of intermolecular interactions below.

We examined three sets of thermostats. All of them have the traditional Nosé–

Copyright © by SIAM. Unauthorized reproduction of this article is prohibited.

Hoover form, with equations of motion given by

$$\frac{dr_{i,\alpha}}{dt} = \frac{p_{i,\alpha}}{m_i}, \tag{4a}$$

$$\frac{dp_{i,\alpha}}{dt} = F_{i,\alpha} - \zeta_{T\alpha} p_{i,\alpha}, \tag{4b}$$

$$\frac{d\zeta_{T\alpha}}{dt} = \frac{\nu_T^2}{f\, k_B T_{set}} \left(\sum_{j=1}^{N} \frac{p_{j,\alpha}^2}{m_j} - f\, k_B T_{set} \right) = \nu_T^2 \left(\frac{T_\alpha(t)}{T_{set}} - 1 \right), \tag{4c}$$

where $r_{i,\alpha}$, $p_{i,\alpha}$, and $F_{i,\alpha}$ are, respectively, the position, momentum, and force of particle i in dimension α; m_i is the mass of particle i; $\zeta_{T\alpha}$ is the scaled thermostat "momentum"; f is the number of degrees of freedom in the system; ν_T is the frequency controlling the rate of thermostat response; and T_{set} is the set temperature. The force contains both the intermolecular component and the contribution from the external field.

The three thermostats are defined as follows. The first thermostat (TS1) has a single thermostat, based on the total kinetic energy of the system; this is the Nosé–Hoover thermostat. In the second thermostat (TS2), we implement spatially localized thermostats by dividing the simulation volume into N_{bin} spatial bins in the z-dimension. The bins are slabs in shape. In this work, $N_{bin} = 50$. A distinct thermostat is assigned to each spatial bin. Equation (4c) is written for each bin, where the relevant kinetic energy and degrees of freedom are those belonging to particles located at that instant within the bin. The thermostat still alters momenta through (4b), with the only extension being that thermostat variable on the left-hand side is from the same bin in which the particle is currently located. In TS2, therefore, as particles move from bin to bin, they move from one thermostat to the next. In the third themostatting scheme (TS3), we implement spatially and dimensionally selective thermostats by providing each of the bins used in TS2 with three thermostats, one for each dimension, resulting in a total of $3N_{bin}$ thermostats. Again, (4b) and (4c) are valid, with the only extension being that the kinetic energy and degrees of freedom used in (4c) correspond to a single dimension.

3. Results and discussion.

3.1. Ideal gas simulations. The purpose of performing ideal gas simulations is strictly to use a simple system where unambiguous analytical results are available. From our simulations we find that all three thermostats satisfy the most basic criterion, namely, that they provide the correct average temperature for the total simulation volume. In Figure 1, we present the temperature profiles for the three thermostats of the ideal gas simulations. In Figure 1, we see that TS1 does not generate the set temperature profile. The failure of TS1 can be explained as follows. The generation of heat due to the inhomogeneous field is spatially nonuniform. In the absence of any temperature control, this will give rise to hot and cold regions in the simulation volume. The single thermostat in TS1 responds only to the average temperature. Therefore, TS1 stops acting when the average temperature reaches the set point temperature. The average set point temperature can be achieved by adjusting the hot and cold regions so that they average to the set temperature, rather than by eliminating the hot and cold regions altogether.

Copyright © by SIAM. Unauthorized reproduction of this article is prohibited.

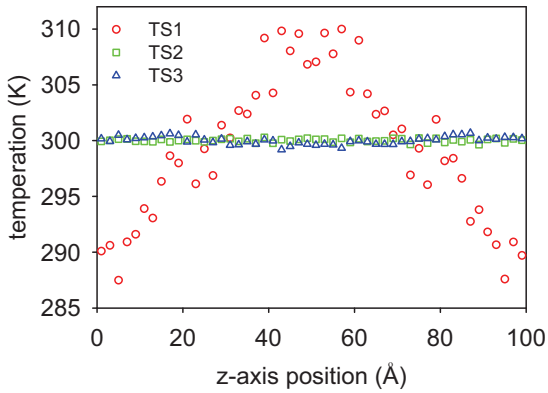

FIG. 1. *Spatial temperature profiles of the ideal gas from MD simulations using three thermostats at* 300 *K: A single thermostat (TS*1*), spatially localized thermostats (TS*2*), and spatially and dimensionally localized thermostats (TS*3*). Both TS*2 *and TS*3 *yield the desired temperature profile.*

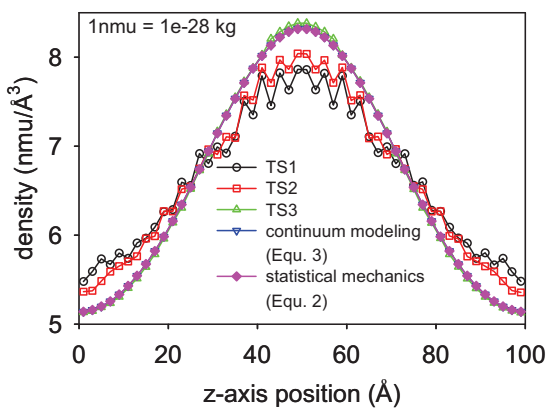

FIG. 2. *Spatial density profiles of the ideal gas from MD simulations using three thermostats at* 300 *K. Also shown are the profiles from statistical mechanics (equation* (2)*) and from the continuum description (equation* (3)*). Only TS*3 *generates the correct profile.*

In both TS2 and TS3, we have spatially selective thermostats. These temperature schemes provide a uniform temperature because the thermostat is based on the local temperature and will act until the local temperature reaches the set point. Based on this evidence alone, one may be inclined to choose TS2 as the optimal thermostat algorithm since it has fewer thermostats. However, validation of the thermostats will provide additional information.

In Figure 2, we present the density profiles from the simulations using TS1, TS2, and TS3. We also plot the statistical mechanical solution in (2) and the continuum solution in (3), where in the latter we used the ideal gas law as the EOS to provide the pressure as a function of density. We see first that, for the case of the ideal gas, the statistical mechanical and continuum solutions are identical. We also observe that only TS3 provides the correct density distribution, despite the fact that both TS2 and TS3 generate correct temperature profiles. TS2 generates the correct temperature profile but the incorrect density distribution because TS2 reacts to a temperature based on the sum of the x-, y-, and z-components of the momentum. The x- and

Copyright © by SIAM. Unauthorized reproduction of this article is prohibited.

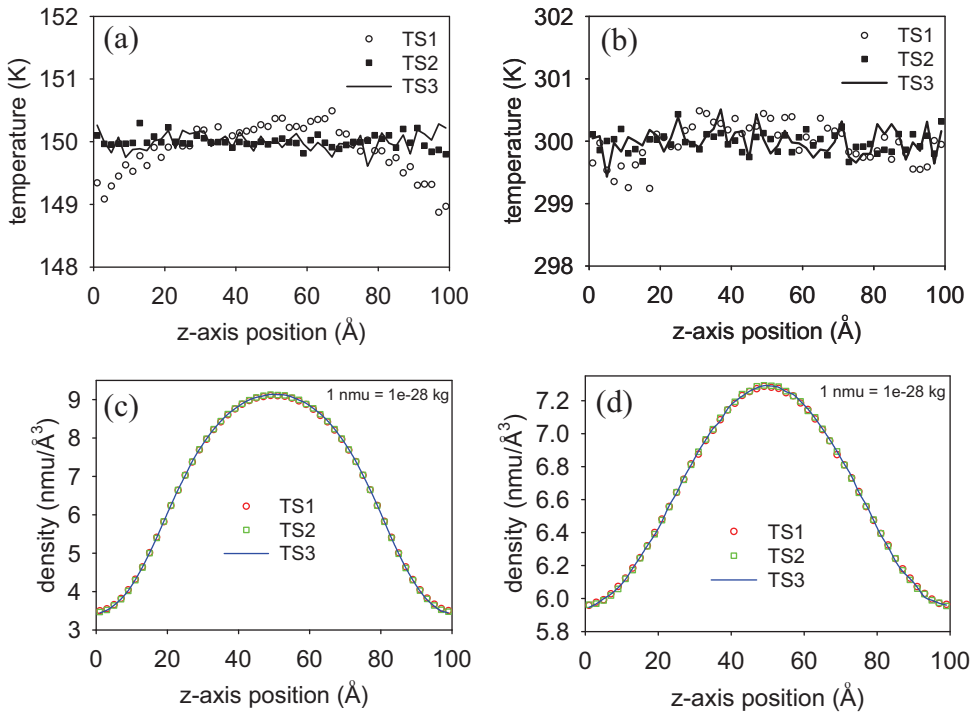

FIG. 3. *Spatial temperature profiles and density profiles of the Lennard–Jones fluid from MD simulations using three thermostats at* 300 *K and* 150 *K:* (a) $T = 150\,K$; (b) $T = 300\,K$; (c) $T = 150\,K$; (d) $T = 300\,K$.

y-components are unaffected by the external potential. However, if the kinetic energy in the z-direction is too high (or too low), the thermostat can reach the set point by lowering (raising) the kinetic energy in all three dimensions. Thus, the z-component of the temperature is still too high (low). Because TS3 has a uniform distribution not only of the sum of the x-, y-, and z-components of the temperature but of each component individually as well, it is capable of generating the correct density profile. At this point, we have established and validated a spatially and dimensionally selective thermostat that correctly generates temperature and density distributions for the ideal gas.

It is worth noting that when an ideal gas is thermostatted with a Nosé–Hoover-type thermostat, the velocities cannot change sign since the thermostat scales the velocities by a positive number [20]. Although the use of multiple thermostats does not solve this pathology, the results of these simulations are not likely affected by it.

3.2. Lennard–Jones fluid simulations. We now perform MD simulations of a fluid with a nonzero intermolecular interaction potential, such as the Lennard–Jones fluid. We performed this MD simulation using TS1, TS2, and TS3, as was the case for the ideal gas. From ideal gas simulations, we know TS3 absolutely can generate a correct temperature and a correct density profile. As we can see from Figure 3, TS1 and TS2 for the Lennard–Jones fluid can also generate a correct density profile compared to TS3, but the temperature profile from TS1 and TS2 is not quite as good as that from TS3. At this point, we can see that the single thermostat is working relatively well for the Lennard–Jones fluid, in which the kinetic energy and poten-

Copyright © by SIAM. Unauthorized reproduction of this article is prohibited.

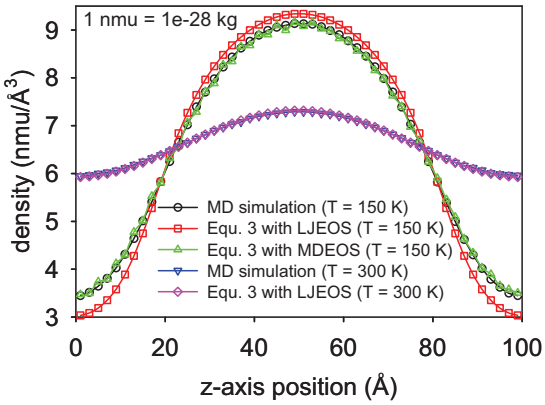

FIG. 4. *Spatial density profiles of the Lennard–Jones fluid from MD simulations using TS3 at* 300 *K and* 150 *K, respectively. Also shown are the profiles from the continuum description with a pressure given by the LJEOS and by* (3)*, compared with the profile from the continuum description with MDEOS and* (3).

tial energy are spatially and dimensionally convertible because of the intermolecular interaction. Then we can use any of the thermostats to generate the density profile for the Lennard–Jones fluid; we used TS3. In Figure 4, we plot the density profile from the MD simulation of the Lennard–Jones fluid. We compare this result with the continuum solution, equation (3), only, since the statistical mechanical result of (2) applies only to the ideal gas. In order to numerically solve (3), we require an accurate EOS for the pressure. We chose two EOSs. The first choice is the Lennard–Jones EOS (LJEOS) [2], which is very accurate in describing the pVT behavior of Lennard–Jones fluids far from the critical point. The LJEOS, when inserted into (3), does a good job of predicting the density distribution at high temperatures but has a systematic error at low temperatures.

The reason for this discrepancy is straightforward. Intermolecular interactions of the type described by the Lennard–Jones potential are nonnegligible on a length scale of 1 nm; in our MD simulations, the potential is truncated at $r_{cut} = 15$ Å. The LJEOS is a bulk EOS because it is based on simulation data of spatially homogeneous fluids. The use of a bulk EOS in the continuum description is justified only when the length scale associated with the variation of density is much larger than the length scale associated with intermolecular interactions. In other words, when the approximation of evaluating the pressure based on the local density is valid, or $p(z) = p_{bulk}(\rho(z))$, a bulk EOS is sufficient. However, in the MD simulations the variation in the density is on the order of nanometers, the same scale as the intermolecular interaction potential. Therefore, a bulk EOS is inadequate, and therein lies the source of the discrepancy between the MD and continuum results. We did not encounter this problem for the ideal gas or the Lennard–Jones fluid at high temperatures because the ideal gas has no intermolecular interactions, and intermolecular interactions have a tiny contribution to the pressure of the Lennard–Jones fluid at high temperatures.

Also shown in Figure 4 is excellent agreement between (3) when the EOS extracted directly from the MD simulation (MDEOS) is inserted. The MDEOS was generated as follows. For each bin, the local pressure of the bin was calculated via published procedures [21]. We calculated the normal pressure (the zz element of the pressure tensor), the tangential pressure (the average of the xx and yy elements), and the

Copyright © by SIAM. Unauthorized reproduction of this article is prohibited.

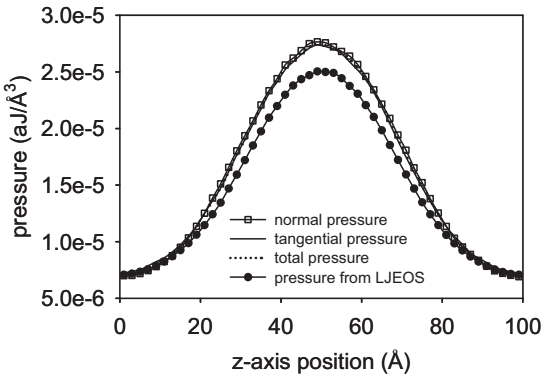

FIG. 5. *Spatial pressure profiles from MD simulation (normal, tangential, and total pressure) and LJEOS at* 150 *K.*

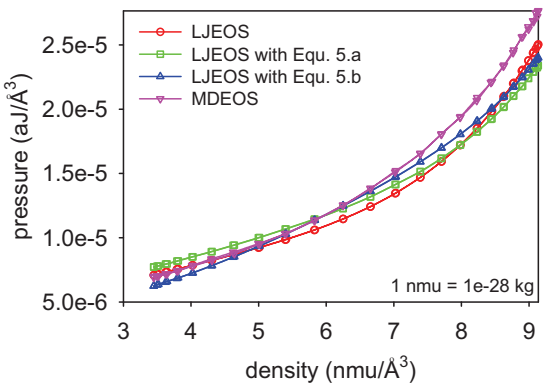

FIG. 6. *Four different equations of state profiles at* 150 *K: LJEOS, locally averaged LJEOS with* (5a)*, locally averaged LJEOS with* (5b)*, and normal pressure calculated from MDEOS.*

average pressure (averaged over all three elements). These pressure profiles are plotted in Figure 5. The LJEOS evaluated at the local density as obtained from the MD simulation is also plotted for reference. There is a significant difference between the MD pressures and the LJEOS pressure. There are small differences (at least in this system) between the normal and tangential components of the pressure tensor. Figure 4 uses the normal component of the pressure tensor. The hydrostatic pressure in (1b) assumed that the diagonal components of the pressure are the same, which is generally not true where there is density variation. (For example, at an interface the surface tension is defined by the difference between the normal and tangential components.)

In Figure 6, we parametrically plot the pressure from Figure 5 versus the density from Figure 4. This is a graphical representation of the mechanical EOS relating pressure to density for this inhomogeneous system. Also on the plot is the LJEOS and what we call a locally averaged LJEOS. We pursued this locally averaged LJEOS to determine if a simple weighting of the bulk LJEOS could approximate the explicit evaluation of the pressure in the MD simulation.

In the locally averaged LJEOS, one can approximate the local pressure in the MD simulation with an average of a bulk EOS evaluated at the local density over the

Copyright © by SIAM. Unauthorized reproduction of this article is prohibited.

cut-off volume,

$$p(z) \approx \frac{\int_{z-r_{cut}}^{z+r_{cut}} p_{bulk}(\rho(\xi))d\xi}{2r_{cut}}. \tag{5a}$$

Alternatively, rather than averaging both the ideal and the nonideal contributions to the pressure, one might argue that a better local average is one in which the ideal contribution is truly local and the nonideal contribution is due to interactions throughout the cut-off volume, in which case only the nonideal contributions are spatially averaged over the cut-off volume,

$$p(z) \approx p_{id}(z) + \frac{\int_{z-rcut}^{z+r_{cut}} (p_{bulk}(\rho(\xi)) - p_{id}(\rho(\xi)))d\xi}{2r_{cut}}. \tag{5b}$$

In Figure 6, we show that the two locally averaged LJEOSs do not provide a good approximation of the MDEOS and are in fact worse than the bulk LJEOS. At this point, we advocate extracting the mechanical EOS directly from the MD simulation as was done here.

4. Conclusions. In this work, we have performed a set of MD simulations in the presence of an anisotropic, inhomogeneous field. We performed simulations of an ideal gas in order to develop and validate a thermostat for MD simulations in the presence of an anisotropic, inhomogeneous field. For the ideal gas, a single Nosé–Hoover thermostat is sufficient to generate the correct average temperature, but the spatial temperature distribution is wrong. Through the use of spatially localized thermostats we were able to generate a desired uniform temperature profile. However, the temperature profile is not sufficient to show that one obtains the correct density distribution. Separate spatially localized thermostats must be used to control the kinetic energy in each dimension in order to account for anisotropy in the external field. For the ideal gas, the use of spatially localized Nosé–Hoover thermostats in each dimension yielded a density distribution that was consistent with both statistical mechanics and a continuum description.

Using this thermostat, we performed MD simulations of a Lennard–Jones fluid in the anisotropic, inhomogeneous field. We generated density and pressure profiles directly from the MD simulation. From this simulation we extracted a mechanical EOS relating pressure to density for this specific system with inhomogeneities in the density on the nanoscale. If we insert this EOS into the continuum-level balances, we find that the solution of these macroscopic equations provides a density distribution that is in complete agreement with that obtained directly from the MD simulations. The use of a bulk EOS in the continuum-level equations does not in general agree with the MD simulations.

In the development of multiscale modeling techniques, one must insist on capturing the important physics at all scales of description. In this work, we show how the conservation of mass and momentum can be consistently described at both the continuum and molecular levels when certain precautions are taken. First, the assumptions must be the same at both levels. If the continuum-level system is assumed to be isothermal, then the molecular-level system must also be isothermal. In this case, we developed a set of thermostats to generate the isothermal condition in the MD simulation. Second, one must use valid constitutive equations. In this case, we extracted an EOS applicable to inhomogeneous fluids directly from the MD simulation. These multiscale modeling techniques will lead to transport properties generated

Copyright © by SIAM. Unauthorized reproduction of this article is prohibited.

by MD simulations in a manner that is completely consistent with continuum-level descriptions of mass transport [22].

REFERENCES

[1] R.B. Bird, W.E. Stewart, and E.N. Lightfoot, *Transport Phenomena*, John Wiley & Sons, New York, 2002.

[2] J.K. Johnson, J.A. Zollweg, and K.E. Gubbins, *The Lennard-Jones equation of state revisited*, Mol. Phys., 78 (1993), pp. 591–618.

[3] H.T. Davis, *Statistical Mechanics of Phases, Interfaces, and Thin Films*, VCH, New York, 1996.

[4] C.Y. Gao, D.M. Nicholson, D.J. Keffer, and B.J. Edwards, *A multiscale modeling demonstration based on the pair correlation function*, J. Non-Newtonian Fluid Mech., 152 (2008), pp. 140–147.

[5] S. Nosé, *A molecular-dynamics method for simulations in the canonical ensemble*, Mol. Phys., 52 (1984), pp. 255–268.

[6] W.G. Hoover, *Canonical dynamics: Equilibrium phase-space distributions*, Phys. Rev. A, 31 (1985), pp. 1695–1697.

[7] K. Cho, J.D. Joannopoulos, and L. Kleinman, *Constant-temperature molecular dynamics with momentum conservation*, Phys. Rev. E, 47 (1993), pp. 3145–3151.

[8] Z. Jia and B.J. Leimkuhler, *A projective thermostatting dynamics technique*, Multiscale Model. Simul., 4 (2005), pp. 563–583.

[9] G.J. Martyna, *Remarks on "constant-temperature molecular dynamics with momentum conservation,"* Phys. Rev. E, 50 (1994), pp. 3234–3236.

[10] J.B. Sturgeon and B.B. Laird, *Symplectic algorithm for constant pressure-molecular dynamics using a Nosé-Poincaré thermostat*, J. Chem. Phys., 112 (2000), pp. 3474–3482.

[11] D.J. Keffer, C. Baig, P. Adhangale, and B.J. Edwards, *A generalized Hamiltonian-based algorithm for rigorous equilibrium molecular dynamics simulation in the canonical ensemble*, J. Non-Newtonian Fluid Mech., 152 (2008), pp. 129–139.

[12] G.J. Martyna, M.L. Klein, and M.E. Tuckerman, *Nose-Hoover chains: The canonical ensemble via continuous dynamics*, J. Chem. Phys., 97 (1992), pp. 2635–2643.

[13] S. Nosé, *A molecular dynamics method for simulations in the canonical ensemble*, Mol. Phys., 52 (1984), pp. 255–268.

[14] M.E. Tuckerman, Y. Liu, G. Ciccotti, and G.J. Martyna, *Non-Hamiltonian molecular dynamics: Generalizing Hamiltonian phase space principles to non-Hamiltonian systems*, J. Chem. Phys., 115 (2001), pp. 1678–1702.

[15] M.E. Tuckerman, C.J. Mundy, and G.J. Martyna, *On the classical statistical mechanics of non-Hamiltonian systems*, Europhys. Lett., 45 (1999), pp. 149–155.

[16] G.S. Heffelfinger and F. van Swol, *Diffusion in Lennard-Jones fluids using dual control-volume grand-canonical molecular dynamics simulation (DCV-GCMD)*, J. Chem. Phys., 100 (1994), pp. 7548–7552.

[17] M.P. Allen and D.J. Tildesley, *Computer Simulation of Liquids*, Oxford Science, Oxford, 1987.

[18] C.W. Gear, *The Numerical Integration of Ordinary Differential Equations of Various Orders*, tech. report, Argonne National Laboratory, Argonne, IL, 1966.

[19] C.W. Gear, *Numerical Initial Value Problems in Ordinary Differential Equations*, Prentice Hall, Englewood Cliffs, NJ, 1971.

[20] G.J. Martyna, M.E. Tuckerman, D.J. Tobias, and M.L. Klein, *Explicit reversible integrators for extended systems dynamics*, Mol. Phys., 87 (1996), pp. 1117–1157.

[21] M.J.P. Nijmeijer, A.F. Bakker, C. Bruin, and J.H. Sikkenk, *A molecular-dynamics simulation of the Lennard-Jones liquid vapor interface*, J. Chem. Phys., 89 (1988), pp. 3789–3792.

[22] D.J. Keffer, C.Y. Gao, and B.J. Edwards, *On the relationship between Fickian diffusivities at the continuum and molecular level*, J. Phys. Chem. B, 109 (2005), pp. 5279–5288.

Copyright © by SIAM. Unauthorized reproduction of this article is prohibited.